biomedicines

MDPI

Systematic Review

CMR-Derived Myocardial Deformation in Autoimmune Rheumatic Diseases: A Systematic Review and Meta-Analysis

Diana-Aurora Arnăutu [1,2,3,†], Masafumi Takafuji [3,4], Sergiu-Florin Arnăutu [1,3,5,6,*], Zaynab Alziyituni [3], Rabeia Javid [3], Chin Soo [3], Thomas Anderton [3], Sebastian Militaru [7,8], Sebastian Onciul [9,10], Raluca Tomoaia [11,12], Ana-Maria Poenar [3], Radu Ioan Lala [13,14], Vlad Morariu [1,2], Brenda Cristiana Bernad [15], Cristian Maghet [2,16], Cristina Văcărescu [17,18,19], Dragoș Cozma [17,18,19], Daniel Malița [20,21,*], Stela Iurciuc [17,22], Minodora Andor [1,2], Octavian Marius Crețu [22,23,†] and Sven Plein [3,24]

1 Department of Internal Medicine, "Victor Babes" University of Medicine and Pharmacy from Timisoara, E. Murgu Sq., No. 2, 300041 Timisoara, Romania; aurora.bordejevic@umft.ro (D.-A.A.)
2 Multidisciplinary Heart Research Center of the "Victor Babes", Internal Medicine Department, University of Medicine and Pharmacy, 300041 Timisoara, Romania
3 Biomedical Imaging Sciences Department, Leeds Institute of Cardiovascular and Metabolic Medicine, University of Leeds, Leeds LS2 9JT, UK
4 Department of Radiology, Mie University Hospital, 2-174 Edobashi, Tsu 514-8507, Mie, Japan
5 Centre for Cognitive Research in Neuropsychiatric Pathology (Neuro-Psy-Cog), Department of Neurosciences, "Victor Babes" University of Medicine and Pharmacy from Timisoara, E. Murgu Sq., No. 2, 300041 Timisoara, Romania
6 Department of Interventional Neuroradiology, Queen's Hospital, Barking, Havering and Redbridge University Hospitals NHS Trust, London RM7 0AG, UK
7 Department of Cardiology, Craiova University of Medicine and Pharmacy, Petru Rareș Street No. 2, 200349 Craiova, Romania
8 Cardiomed Hospital, Str. Spania, Nr. 35A, 200513 Craiova, Romania
9 Faculty of Medicine, "Carol Davila" University of Medicine and Pharmacy, 020021 Bucharest, Romania
10 Department of Cardiology, Floreasca Emergency Clinical Hospital, 014461 Bucharest, Romania
11 4th Department of Internal Medicine, Faculty of Medicine, "Iuliu Haţieganu" University of Medicine and Pharmacy, 400347 Cluj-Napoca, Romania
12 Department of Cardiology, Heart Institute "N. Stăncioiu", 400001 Cluj-Napoca, Romania
13 Department of Cardiology, "Vasile Goldis" Western University, 310025 Arad, Romania
14 Department of Cardiology, Arad Western University Vasile Goldis, 310414 Arad, Romania
15 Center for Neuropsychology and Behavioral Medicine, "Victor Babeș" University of Medicine and Pharmacy, 300041 Timisoara, Romania
16 Center for Diagnosis and Study of Parasitic Diseases, Department of Infectious Diseases, "Victor Babes" University of Medicine and Pharmacy, 300041 Timisoara, Romania
17 Cardiology Department, "Victor Babes" University of Medicine and Pharmacy, 2 Eftimie Murgu Sq., 300041 Timisoara, Romania
18 Research Center of the Institute of Cardiovascular Diseases Timisoara, 13A Gheorghe Adam Street, 300310 Timisoara, Romania
19 Institute of Cardiovascular Diseases Timisoara, 13A Gheorghe Adam Street, 300310 Timisoara, Romania
20 Department XV, Clinic of Radiology and Medical Imaging, "Victor Babeș" University of Medicine and Pharmacy, 300041 Timisoara, Romania
21 Department of Radiology and Medical Imaging, "Pius Brînzeu" Emergency County Hospital, 300723 Timisoara, Romania
22 Municipal Emergency Clinical Hospital Timișoara, 300041 Timisoara, Romania
23 Department of Surgery I, Division of Surgical Semiology I, "Victor Babes" University of Medicine and Pharmacy, Eftimie Murgu Sq. No. 2, 300041 Timisoara, Romania
24 Department of Cardiology, Leeds General Infirmary, Leeds Teaching Hospitals NHS Trust, Great George Street, Leeds LS1 3EX, UK
* Correspondence: arnautu.sergiu@umft.ro (S.-F.A.); d.malita@gmail.com (D.M.)
† These authors contributed equally to this work.

Check for updates

Academic Editor: Amedeo Amedei

Received: 14 October 2026
Revised: 12 November 2026
Accepted: 13 November 2026
Published: 18 November 2026

Copyright: © 2026 by the authors. Licensee MDPI, Basel, Switzerland. This article is an open access article distributed under the terms and conditions of the Creative Commons Attribution (CC BY) license.

Abstract

Background/Objectives: We assessed cardiovascular magnetic resonance (CMR)-derived myocardial deformation in autoimmune rheumatic diseases (ARDs), distinguishing cohorts with documented absence of clinically overt cardiac involvement from incompletely documented and broader clinical populations. **Methods**: The original searches of PubMed,

Embase, Scopus, and CENTRAL were performed on 2 September 2026. Web of Science and supplementary citation searching were added during revision, with final search exports dated 27 October 2026. Principal random-effects analyses used cohorts with documented target phenotypes and direct mean/SD data, restricted maximum likelihood estimation and ordinary Hartung–Knapp inference; modified Hartung–Knapp inference was examined as a sensitivity analysis. Critical appraisal used JBI tools and certainty was assessed using GRADE. PROSPERO: CRD420261495586. **Results**: We retained 73 reports in 48 cohort families. In the principal GLS analysis, five comparisons involving 168 patients and 130 controls gave a mean difference of 2.46 percentage points (95% CI 0.82 to 4.11), indicating less negative GLS in the disease groups. The 95% prediction interval included zero (−1.33 to 6.26). The confidence intervals for global circumferential and radial strain included differences in both directions. Evidence certainty was very low for all three outcomes. **Conclusions**: The pooled GLS estimate suggested a smaller magnitude of longitudinal shortening in patients with autoimmune rheumatic diseases without established clinically overt cardiac disease, but the evidence was very uncertain. The evidence for circumferential and radial strain was also very uncertain.

Keywords: cardiovascular magnetic resonance; CMR; myocardial strain; global longitudinal strain; autoimmune rheumatic disease; systemic sclerosis; systemic lupus erythematosus; feature tracking; subclinical cardiac dysfunction; myocardial deformation

1. Introduction

Autoimmune rheumatic diseases (ARDs) comprise a heterogeneous group of chronic systemic inflammatory disorders that may involve the myocardium, coronary microcirculation, pericardium, valves, conduction system, and pulmonary vasculature. Cardiovascular involvement contributes substantially to morbidity and mortality, yet myocardial disease may remain clinically silent for prolonged periods and precede abnormalities in conventional indices, such as left ventricular ejection fraction (LVEF) [1,2]. Speckle-tracking echocardiography, particularly the assessment of left ventricular global longitudinal strain (GLS), has emerged as a sensitive method for detecting subclinical myocardial dysfunction despite preserved LVEF. In systemic sclerosis, a recent systematic review and meta-analysis by Casian et al. demonstrated impaired myocardial deformation, supporting the incremental value of strain imaging in identifying early cardiac involvement that may not be apparent on conventional echocardiography [3].

Conventional echocardiographic and CMR measures of global systolic function may underestimate early myocardial injury. Cardiovascular magnetic resonance provides comprehensive tissue characterisation and highly reproducible quantification of ventricular volumes and function, while CMR-derived myocardial deformation techniques provide additional information on myocardial mechanics. Feature tracking can quantify longitudinal, circumferential, and radial strain from routinely acquired cine images, whereas myocardial tagging and other dedicated deformation techniques offer alternative approaches to regional and global myocardial mechanics [4].

Global longitudinal strain (GLS) may be particularly relevant to early myocardial involvement because longitudinal deformation reflects myocardial fibre architecture and may become abnormal before overt reduction in LVEF [3]. Individual studies have reported abnormal CMR-derived strain in systemic sclerosis (SSc) [5–9], systemic lupus erythematosus (SLE) [10–12], rheumatoid arthritis (RA) [13], primary Sjögren syndrome (pSS) [14] and idiopathic inflammatory myopathies (IIM) [15]. However, available studies are generally

small, use different scanners and post-processing software, and vary in their definitions of global, regional and single-view deformation.

Consequently, it remains unclear which CMR-derived deformation components show the most reproducible abnormalities across ARDs and whether apparent differences are robust to methodological choices, including conversion of non-parametrically reported data and inclusion of limited-view measurements.

Previous echocardiographic syntheses have demonstrated impaired ventricular and atrial strain in systemic sclerosis, whereas CMR additionally permits deformation assessment alongside myocardial tissue characterisation with LGE and parametric mapping. The present review therefore focuses specifically on CMR-derived deformation across autoimmune rheumatic diseases rather than reproducing the existing speckle-tracking echocardiography evidence base [3,16].

The primary objective of this systematic review and meta-analysis was to quantify differences in CMR-derived LV GLS between patients with ARDs with documented absence of clinically overt cardiac involvement and healthy controls. Secondary objectives were to evaluate LV global circumferential strain (GCS), LV global radial strain (GRS), right ventricular deformation, atrial deformation, myocardial strain rate and regional deformation, while accounting explicitly for differences in population phenotype and measurement definition. Review-level eligibility was distinguished from eligibility for individual quantitative syntheses, with incompletely documented and broader clinical populations evaluated separately from the principal target population.

2. Materials and Methods

2.1. Protocol, Registration, and Reporting

The review protocol was submitted to PROSPERO on 2 September 2026 and registered on 3 September 2026 (CRD420261495586). The original database search is dated 2 September 2026 in the search ledger. The PROSPERO record indicated that pilot work, formal searching and eligibility screening had started. The retained records do not establish the date of the first formal eligibility decision. The search was expanded and updated in October 2026. Reporting followed PRISMA 2020 [17]. Revision-stage decisions included restriction of the principal analyses to documented target phenotypes and direct mean/SD data, a minimum of three comparable cohort contributions for pooling, additional sensitivity analyses, and clarification of the GRADE certainty target. These changes are reported as revision-stage decisions rather than retrospectively described as prespecified.

Revision-Stage Deviations and Clarifications

During revision, we broadened the database search strategies, added Web of Science, and conducted forward citation searching in addition to backward reference checking. The registered search plan stated, “Only published studies will be sought.” The preceding revision included a Research Square preprint identified through citation searching. We excluded this report from the revised evidence set and refitted the affected models. The report did not establish whether the strain measures were global, and the strain analysis software was unspecified. The supplementary amendment table documents the search changes, the English-language restriction applied during full-text assessment, the revised requirements for the principal analyses, and the change from two to three comparable contributions for pooling. Supplementary Table S5 documents the amendments to the registered review methods, including the addition of the exploratory prognostic and longitudinal treatment scopes.

2.2. Eligibility Criteria

The review targeted adults aged ≥18 years with eligible autoimmune rheumatic diseases and quantitative myocardial deformation assessed using CMR. Eligible techniques included feature tracking, tissue tracking, myocardial tagging, displacement encoding with stimulated echoes, strain-encoded imaging and other relevant CMR-based deformation methods. A healthy comparator was required for the principal disease–control meta-analyses. Eligible within-disease, prognostic and treatment comparisons were considered in separate secondary scopes. Standalone conference abstracts were eligible when they provided sufficient information to establish review eligibility. Their contribution to individual syntheses was assessed separately using the outcome-specific data requirements.

Reports assessing deformation exclusively using non-CMR methods, or reporting CMR volumes, ejection fraction, LGE or mapping without eligible deformation measurements, were excluded. Insufficient data for a particular pooled outcome did not automatically exclude a report that supplied other eligible information. Related reports could be retained when they contributed complementary information.

Minimum-age documentation was recorded explicitly. Where the available report did not establish the minimum age, this uncertainty was retained and examined in a sensitivity analysis restricted to explicitly verified adult-age data; incomplete reporting was not treated as verification that every participant was aged ≥18 years.

Principal and Broader Population Evidence

Review-level eligibility and eligibility for each quantitative synthesis were assessed separately. Clinical phenotype was classified as documented absence of clinically overt cardiac involvement (D), incompletely documented target phenotype (U), or broader clinical involvement (B). Principal models required the documented target phenotype, an eligible healthy comparator, compatible measurement definitions and usable direct mean/SD data. Expanded analyses combined otherwise eligible D, U, and B contributions and were interpreted as secondary analyses addressing a broader population scope.

Clinical presentation, LVEF, and myocardial tissue findings were considered separately. Preserved LVEF or absence of LGE alone did not establish the target clinical phenotype. Reports could remain included while particular outcomes were withheld or assigned to a separate synthesis. Publication type, comparator eligibility, age documentation and possible cohort overlap were recorded explicitly.

2.3. Information Sources and Search Strategy

The original searches covered PubMed, Embase via Ovid, Scopus, and the Cochrane Central Register of Controlled Trials (CENTRAL). During revision, we broadened the database search strategies, added Web of Science and supplemented backward reference checking with forward citation searching. The final database exports were dated 27 October 2026. The updated records were rescreened, and the report-level adjudication for that search update was recorded on 1 November 2026.

Search terms covered cardiovascular magnetic resonance, myocardial strain and deformation, relevant measurement techniques, and individual autoimmune rheumatic diseases. The supplementary search record provides database-specific strategies, interfaces, available search and export dates, and citation search methods.

The database searches had no language restriction. During revision, we introduced an English-language restriction at full-text assessment and excluded one report on this basis. The registered protocol did not specify this full-text restriction. The supplementary amendment table and full-text exclusion register document the decision and identify the excluded report.

2.4. Screening, Eligibility, and Cohort-Family Management

S.F.A. and D.A.A. independently screened records using the same eligibility criteria and then compared their final decisions. AI-assisted eligibility assessments were used as supporting material. S.F.A. and D.A.A. made the final inclusion and exclusion decisions. Rayyan was used to manage screening. We recorded one primary exclusion reason for each report excluded after full-text assessment. Reports that could not be retrieved were recorded separately.

Related publications were linked as possible cohort families. Companion reports could be retained if they supplied relevant additional information. Within each model, one compatible contribution per conservative cohort family was selected to avoid double counting. A shared author group alone was not treated as proof of identical participants. Where substantial cohort overlap was considered highly likely on the basis of centre, investigators, recruitment population, methodology, sample size and study question, related reports were linked conservatively; the later or more complete report was selected for a common endpoint when the earlier report supplied no additional eligible information. Full-report exclusion reasons and reports that could not be retrieved are provided separately in the supplement.

2.5. Data Extraction

The data were organised in a structured outcome-level workbook using machine-assisted preparation. The retained records do not consistently identify who originally extracted each numerical input. During revision, AI assistance was used to support source cross-checking, data reconciliation and numerical checks. During this revision, S.F.A. checked the outcome definitions, time points, group sizes, means and standard deviations for 13 principal strain comparisons and five contextual LVEF comparisons against the original reports and their supplements. D.A.A. reviewed the completed verification log, which records the published source location and the result of each check. Extracted information included study design, disease, population characteristics, group denominators, clinical phenotype, LVEF, LGE, CMR acquisition and analysis methods, outcome definitions, original summary statistics, and source locations. Cohort family links and outcome-specific numerical admission decisions were recorded.

The verification log identifies previously documented checks by the authors. Computational validation checked linkage to the retained report roster, unique cohort contributions within models, sampling variances and reproduction of the ordinary and modified Hartung–Knapp calculations. Computational validation and author consensus on eligibility were not treated as evidence of additional independent human numerical verification.

Outcomes with unresolved numerical inconsistencies, incompatible or unresolved units, nonseparable eligible populations, or insufficient comparator information were withheld from the affected synthesis. No unverified correction was imposed.

2.6. Harmonisation of Myocardial Deformation Outcomes

LV GLS was the primary outcome. Secondary families comprised LV GCS and GRS, right ventricular and atrial deformation, strain-rate components and regional myocardial deformation. Only sufficiently comparable measurements were pooled. Explicit three-dimensional, regional, tagging, restricted-view and annular measurements were maintained in separate scopes.

Mean differences were calculated as disease minus control. Positive differences for conventionally negative GLS and GCS indicate less negative strain in the disease group; negative radial strain differences indicate lower radial deformation. Documented positive-magnitude GLS/GCS measurements were converted to the signed convention by

negating group means while retaining SDs. No automatic sign reversal was applied to unrelated outcomes.

Strain was expressed in percentage points and compatible strain rates in s^{-1}. Unresolved scales were withheld without an assumed factor-of-100 correction.

2.7. Management of Non-Normally Reported Data and Shared Controls

Principal LV models used directly reported or appropriately combined mean/SD data. Median/IQR-derived observations were restricted to explicitly labelled sensitivity analyses. Means were estimated using the Luo S2 method [18] and SDs using the finite-sample IQR method of Wan et al. [19]. Original quartiles and the calculation audit were retained.

Directly reported disease subgroups sharing one control group were combined using within- and between-subgroup variability before analysis, so that the same controls were counted once. This procedure was distinguished from median/IQR conversion. Internally inconsistent values were not silently corrected.

2.8. Methodological Quality Assessment

Critical appraisal used the 2017 JBI analytical cross-sectional checklist for eligible baseline comparisons, with separate cohort and quasi-experimental checklists for prognostic and treatment components [20]. Responses were recorded as Yes, No, Unclear or Not Applicable. No summed quality score or arbitrary score-based exclusion threshold was used.

AI-assisted item-level proposals were used during the initial review to prepare preliminary judgements and identify relevant source passages. During revision, AI assistance also supported source-based appraisal. Section 3.3 and the supplementary appraisal register describe the available reviewer records and supporting evidence. An Unclear judgement indicates that the source report provided insufficient information to answer the appraisal question.

2.9. Statistical Analysis

Analyses were performed in R version 4.6.1 using metafor version 5.0-1 [21]. Separate random-effects models were fitted for each compatible outcome and population scope. Between-study variance was estimated using restricted maximum likelihood. Ordinary Hartung–Knapp inference with t-based confidence intervals was the primary method [22]. Modified Hartung–Knapp inference, imposing a lower bound of one on the HK scale factor, was evaluated as a sensitivity analysis [23].

Heterogeneity was described using Cochran's Q, I^2 and τ^2, with Q-profile confidence intervals for τ^2. The main results report prediction intervals using $k-2$ degrees of freedom. The supplement provides the $k-1$ calculation using the same variance term.

The revised analysis policy required at least three comparable cohort family contributions for pooling. With fewer than three, individual estimates were displayed without a pooled result. Principal analyses required documented target phenotypes and direct mean/SD data. Sensitivity analyses considered median/IQR conversion, phenotype expansion, alternative cohort representatives and comparators, publication type, age documentation, LGE restrictions, standardised effects, and leave-one-out omission. Standardisation using Hedges' g did not establish interchangeability of measurement platforms or constructs.

Exploratory funnel plots and Egger-type mixed-effects regression on standard error were evaluated for expanded direct-data GLS, GCS and GRS models containing at least 10 contributions. These diagnostics were not applied to the principal models, each of

which contained fewer than 10 comparisons. Nonsignificant tests were not taken to exclude publication bias.

The *p*-values were descriptive. Interpretation considered effect estimates, confidence intervals, prediction intervals, heterogeneity, sensitivity analyses and the specified certainty target.

2.10. Certainty of Evidence Assessment

We assessed certainty separately for each outcome and comparison using GRADE [24–26]. For disease–control comparisons, we rated certainty in the direction of the average unadjusted association between disease status and each left ventricular strain outcome, using zero as the threshold. We followed the association framework described by Brignardello-Petersen and Guyatt [26] and began at high certainty because observational comparisons are an appropriate design for this descriptive question. We assessed risk of bias, inconsistency, indirectness, imprecision and publication bias separately. Evidence for treatment effects started at low certainty. The association-specific framework and the use of zero as the threshold were clarified during revision.

We assessed imprecision using the modified Hartung–Knapp confidence interval for the pooled average. The main statistical results use ordinary Hartung–Knapp inference, with modified intervals reported separately. Prediction intervals informed the interpretation of variation across settings. We assessed incomplete documentation of adult eligibility under indirectness because the registered target population was adults aged 18 years or older. We based each risk-of-bias judgement on the reports contributing to the outcome and their item-level appraisals. The supplementary GRADE profiles document the rationale for each judgement.

3. Results

3.1. Search and Study-Selection Results

The updated database searches identified 4857 records; 2058 duplicates were removed, leaving 2799 records. Citation searching identified 1523 records; after removal of 390 duplicates within the citation results and 96 records already present in the database set, 1037 additional records remained. In total, 3836 records were screened, and 3421 were excluded at title/abstract assessment.

After title and abstract screening, 415 records were forwarded for retrieval, including 197 from database searches and 218 identified only through citation searching. Six linked records or assets were consolidated, and one author-identified report was added, yielding 410 reports sought for retrieval. Of these, 27 could not be retrieved. The retained retrieval records do not establish whether study authors were contacted or interlibrary loan was requested for these 27 reports. We assessed 383 reports for eligibility, excluded 310, and retained 73 reports in 48 cohort families. The supplementary study selection register lists the primary reason for each full-text exclusion.

3.2. Study Characteristics and Synthesis Coverage

The principal GLS analysis included five comparisons across four disease categories, with two comparisons in idiopathic inflammatory myopathy and one each in rheumatoid arthritis, systemic lupus erythematosus, and systemic sclerosis. Four of these comparisons contributed to both the GCS and GRS analyses. Table 1A summarises the clinical characteristics of the five contributing reports. Table 1B presents their study designs, scanner field strengths, strain techniques and analysis software. The characteristics of all retained reports, endpoint-specific membership, denominators and cohort family decisions are provided in the Supplementary Materials. Participant totals are presented by outcome and are not

summed across outcomes (Figure 1). Additional outcome and sensitivity forest plots are presented in Figures S1–S25.

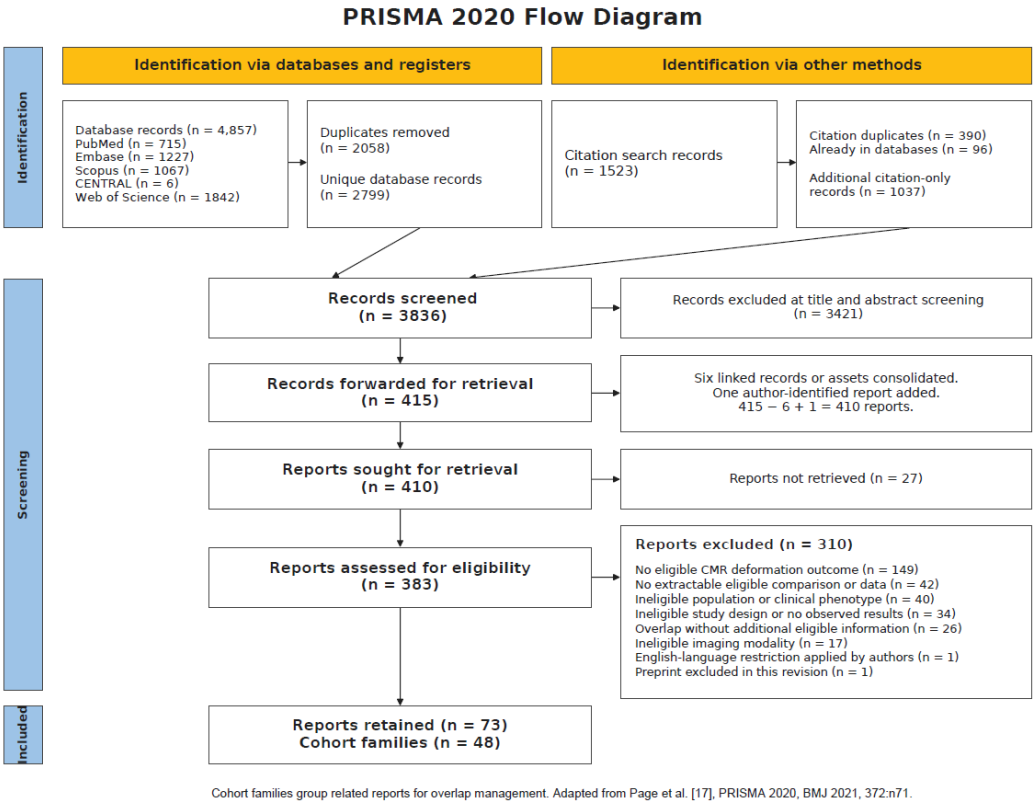


Figure 1. PRISMA 2020 [17] flow diagram of study identification and selection. We screened 3836 records, sought 410 reports, and assessed 383 for eligibility. After 310 full-text exclusions, 73 reports were retained in 48 cohort families. One additional report, Treiber et al. (2026) [27], was identified by the authors, assessed for full-text eligibility, and retained. Adapted from Page et al. [17].

Table 1A,B summarizes, respectively, the clinical characteristics and CMR methodology of the reports contributing to the principal left ventricular strain analyses.

Table 1. (**A**) Clinical characteristics of the studies contributing to the principal left ventricular strain analyses. (**B**) Study design and CMR methods for the principal left ventricular strain analyses.

(**A**)

Report	Disease	n, Patients/ Controls	Age, Years, mean ± SD	Female, n/N (%)	LVEF, %, mean ± SD	LGE, n/N	Outcomes
Kersten et al., 2021 [15]	IIM	47/25	54.3 ± 15.4/ 53.4 ± 10.75	25/47 (53.2%)/13/25 (52.0%)	66.6 ± 6.2/ 62.0 ± 5.6	28/47/0/25	GLS, GCS, GRS
Zhao et al., 2021 [28]	IIM	30/30	41.5 ± 15.4/ 40.6 ± 14.2	24/30 (80.0%)/20/30 (66.7%)	64.1 ± 6.4/ 62.0 ± 7.8	0/30/0/30 by selection	GLS, GCS, GRS
Tański et al., 2021 [13]	RA	30/26	49.83 ± 13.68/ 49.42 ± 7.16	20/30 (66.7%)/16/26 (61.5%)	63.62 ± 7.39/ 63.46 ± 5.28	Not acquired	GLS, GCS, GRS
Puntmann et al., 2013 [12]	SLE	33/21	40 ± 8/38 ± 6	26/33 (78.8%)/16/21 (76.2%)	59 ± 5/61 ± 5	20/33/0/21	GLS, GCS, GRS
Ross et al., 2022 [7]	SSc	28/28	55.10 ± 7.54/ 56.32 ± 9.66	23/31 (74.2%)/23/31 (74.2%)	64.38 ± 6.37/ 61.09 ± 5.06	9/30/0/30	GLS

Table 1. *Cont.*

(**B**)

Report	Study Design and Comparison	Field Strength and Scanner	Strain Technique	Strain Software
Kersten et al., 2021 [15]	Observational study with longitudinal follow-up. The principal analyses used the baseline comparison with age- and sex-matched healthy volunteers.	1.5 T, Philips Intera	Cine CMR feature tracking	cmr42 (Circle Cardiovascular Imaging)
Zhao et al., 2021 [28]	Single-centre retrospective case–control study with age- and sex-matched healthy controls	3 T, Siemens MAGNETOM Skyra	Cine CMR feature tracking	cvi42 (Circle Cardiovascular Imaging)
Tański et al., 2021 [13]	Prospective observational study with a cross-sectional comparison of patients with rheumatoid arthritis and controls	1.5 T, Siemens MAGNETOM Aera	Cine CMR feature tracking	QStrain RE (Medis Suite MR, Medis)
Puntmann et al., 2013 [12]	Cross-sectional comparison of patients with systemic lupus erythematosus and controls	3 T, Philips Achieva	Two-dimensional cine CMR feature tracking	TomTec prototype software (TomTec GmbH)
Ross et al., 2022 [7]	Observational study with a cross-sectional comparison against age- and sex-matched controls	3 T, Siemens MAGNETOM Prisma	Cine CMR feature tracking	cvi42 (Circle Cardiovascular Imaging)

(**A**) Note: Values are presented for patients and controls, respectively. Group sizes refer to the strain comparisons. For Ross et al., Supplementary Table S2 (printed page 4) reports GLS for 28 participants per group, age, sex and LVEF for 31 per group, and LGE for 30 per group. Mean GLS was −16.68% (SD 2.31) in patients and −20.30% (SD 3.41) in controls. The source does not explain why fewer participants had GLS data. Full characteristics of the 73 retained reports are provided in the Supplementary Materials. IIM, idiopathic inflammatory myopathy. RA, rheumatoid arthritis. SLE, systemic lupus erythematosus. SSc, systemic sclerosis. LVEF, left ventricular ejection fraction. LGE, late gadolinium enhancement. (**B**) CMR, cardiovascular magnetic resonance. Strain software was extracted from the original reports and, for Ross et al. [7], from the supplementary CMR methods.

3.3. Methodological Quality

Baseline analytical cross-sectional appraisal covered 68 of the 73 retained reports and yielded 544 item-level judgements, comprising 419 Yes, seven No, and 118 Unclear responses. Three reports were appraised only with a design-specific checklist. Two retained companion reports had no baseline appraisal because the exact primary sources were unavailable. Design-specific appraisal of six cohort and six quasi-experimental components yielded 120 item-level judgements, comprising 68 Yes, 14 No, 34 Unclear, and four Not Applicable responses.

The appraisal register contained previously recorded reviewer consensus for 328 baseline items across 41 reports. During this revision, S.F.A. and D.A.A. confirmed that, for the remaining 216 baseline items across 27 reports, both reviewers' ratings agreed with the AI-assisted source judgements. This confirmation was added to the register, which now records reviewer consensus for all 544 assessed baseline items. For the 120 design-specific items, the register contains AI-assisted source judgements, with no individual reviewer ratings or consensus recorded. The supplementary appraisal register provides the item-level judgements, supporting evidence and provenance.

3.4. Primary Outcome: Left Ventricular Global Longitudinal Strain

Five comparisons involving 168 patients and 130 controls contributed to the principal GLS analysis. GLS was less negative in the disease groups by 2.46 percentage points (ordinary and modified Hartung–Knapp 95% CI 0.82 to 4.11). The 95% prediction intervals included zero (−1.33 to 6.26 using k−2 and −0.85 to 5.77 using k−1). Leave-one-out point estimates ranged from 2.15 to 2.83 percentage points. After omitting Puntmann et al. [12], the confidence interval included zero (MD 2.35, 95% CI −0.07 to 4.77). Supplementary

Table S3 presents the pooled mean differences and the ordinary and modified Hartung–Knapp 95% confidence intervals for all five leave-one-out analyses. The corresponding standardised difference was Hedges' $g = 0.80$ (95% CI 0.33 to 1.26).

The contextual LVEF analysis included 171 patients and 133 controls. Ross et al. contributed three more observations per group for LVEF than for GLS (Figure 2). The LVEF mean difference was 1.63 percentage points (ordinary Hartung–Knapp 95% CI −1.69 to 4.95).

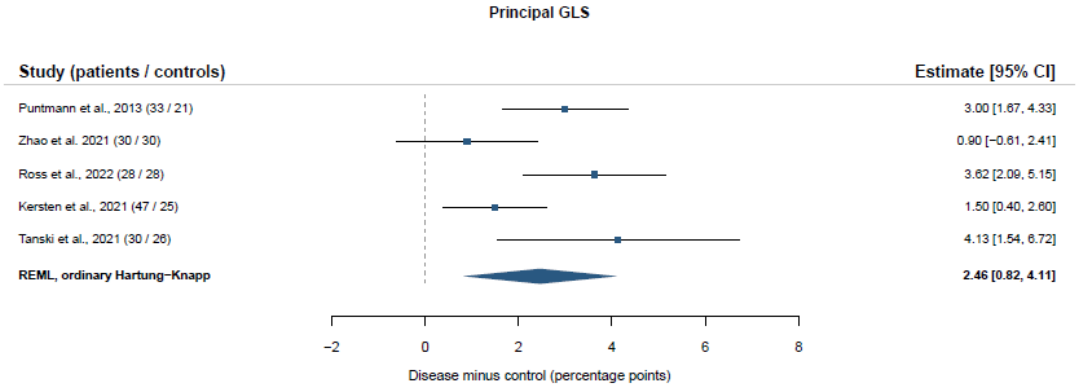


Figure 2. Principal meta-analysis of left ventricular global longitudinal strain (five comparisons; 168 patients and 130 controls) [7,12,13,15,28]. Positive disease-minus-control mean differences indicate less-negative GLS in the disease groups. Squares represent individual study estimates, with their size reflecting study weight; horizontal lines indicate 95% confidence intervals. The diamond represents the pooled estimate and its 95% confidence interval, and the vertical dotted line indicates the null value. Bold text identifies the column headings and pooled result. The pooled estimate uses ordinary Hartung–Knapp inference.

3.5. Left Ventricular Global Circumferential Strain

Four comparisons involving 140 patients and 102 controls gave a GCS mean difference of 0.91 percentage points (ordinary Hartung–Knapp 95% CI −1.31 to 3.12, modified Hartung–Knapp 95% CI −1.38 to 3.19). The corresponding standardised difference was Hedges' $g = 0.26$ (95% CI −0.33 to 0.85) (Figure 3).

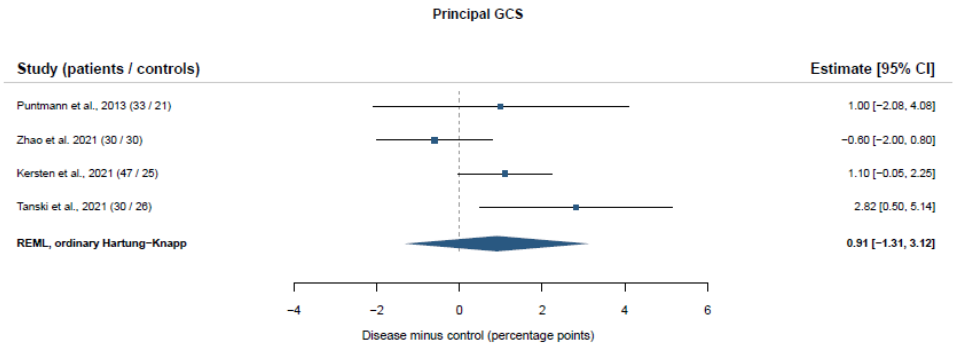


Figure 3. Principal meta-analysis of left ventricular global circumferential strain (four comparisons; 140 patients and 102 controls) [12,13,15,28]. Positive disease-minus-control mean differences indicate less-negative GCS in the disease groups. Squares represent individual study estimates, with their size reflecting study weight; horizontal lines indicate 95% confidence intervals. The diamond represents the pooled estimate and its 95% confidence interval, and the vertical dotted line indicates the null value. Bold text identifies the column headings and pooled result. The pooled estimate uses ordinary Hartung–Knapp inference.

3.6. Left Ventricular Global Radial Strain

Four comparisons involving 140 patients and 102 controls gave a GRS mean difference of −1.42 percentage points (ordinary Hartung–Knapp 95% CI −4.80 to 1.96, modified Hartung–Knapp 95% CI −5.27 to 2.43). The corresponding standardised difference was Hedges' $g = -0.14$ (95% CI −0.52 to 0.25) (Figure 4).

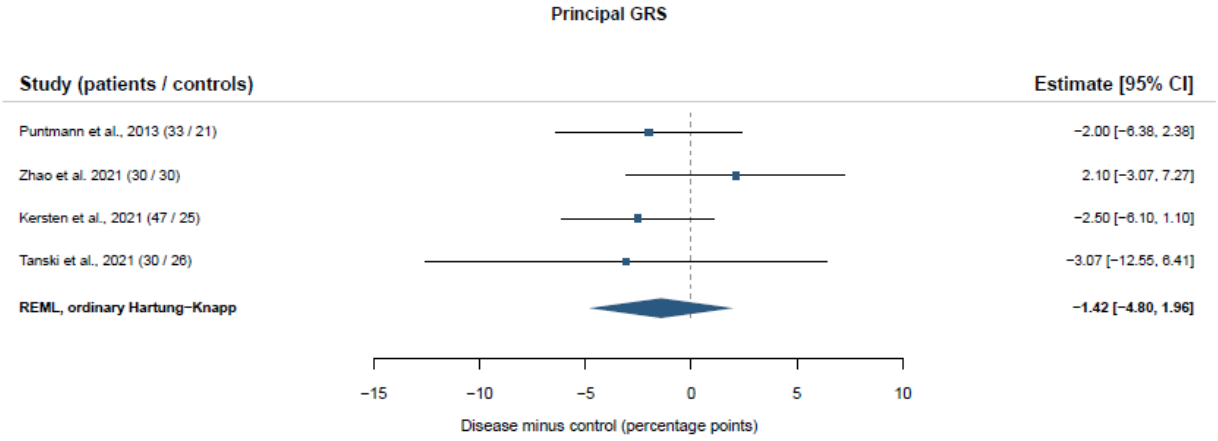


Figure 4. Principal meta-analysis of left ventricular global radial strain (four comparisons; 140 patients and 102 controls) [12,13,15,28]. Negative disease-minus-control mean differences indicate lower GRS in the disease groups. Squares represent individual study estimates, with their size reflecting study weight; horizontal lines indicate 95% confidence intervals. The diamond represents the pooled estimate and its 95% confidence interval, and the vertical dotted line indicates the null value. Bold text identifies the column headings and pooled result. The pooled estimate uses ordinary Hartung–Knapp inference.

3.7. Expanded-Population Left Ventricular Analyses

Expanded direct-data analyses combined cohorts with documented, incompletely documented, and broader clinical phenotypes. The pooled mean differences were 1.97 percentage points for GLS (14 comparisons, 95% CI 0.86 to 3.07), 1.13 for GCS (nine comparisons, 95% CI 0.48 to 1.78), and −5.65 for GRS (10 comparisons, 95% CI −10.21 to −1.10). The corresponding 95% prediction intervals using k−2 degrees of freedom were −1.86 to 5.80, 0.06 to 2.20, and −18.49 to 7.18, respectively (Figures S3, S8 and S13).

The two LGE-negative GLS comparisons gave mean differences of 0.40 percentage points for Kersten et al. [15] (95% CI −0.91 to 1.71, 19 patients and 25 controls) and 0.90 for Zhao et al. (2021) [28] (95% CI −0.61 to 2.41, 30 patients and 30 controls). Restriction to explicitly verified adult eligibility left one GLS comparison, Ross et al. [7] (MD 3.62 percentage points, 95% CI 2.09 to 5.15, 28 patients and 28 controls). Supplementary Table S4 presents the individual estimates for the two LGE-negative comparisons and the one comparison with explicitly verified adult eligibility. Neither restriction met the minimum of three comparisons for pooling.

3.8. Left Ventricular Strain-Rate Outcomes

Strain-rate evidence remained sparse and definition-dependent. Under the revised pooling policy, outcomes with fewer than three compatible contributions were displayed individually. In the documented-phenotype analyses augmented with eligible conversions, five strain-rate models contained three contributions, while systolic longitudinal strain rate had only two and was not pooled.

Zhao et al. (2021) [28] and Huang L et al. (2025) [10] contributed to all six left ventricular strain-rate analyses. Peng et al. (2026) [6] also contributed to the systolic and

diastolic circumferential and radial analyses, and Yokoe et al. (2021) [14] contributed to the diastolic longitudinal analysis. After excluding converted inputs flagged for quartile asymmetry, diastolic longitudinal and systolic circumferential strain rate fell below the minimum of three compatible contributions for pooling.

Diastolic radial strain rate had an ordinary-HK MD of −0.034 s^{-1} (95% CI −0.064 to −0.004), but its modified-HK interval crossed zero (−0.339 to 0.271; $p = 0.679$). No directional conclusion was robust to modified-HK sensitivity across these strain-rate models. Limited-view and regional measurements were retained in separate scopes (Figures S16–S21).

3.9. Right Ventricular, Right Atrial and Regional Deformation

The available data did not support pooled estimates for right ventricular or right atrial deformation. Compatible right ventricular comparisons were sparse, and right atrial rows were held, used a separate comparator, or did not provide a separable eligible population. Individual findings were therefore reported without aggregate right-heart inference.

Regional, tagging, restricted-view, annular, and explicit three-dimensional measurements were maintained as separate outcomes. Their source definitions, population scope and numerical availability are detailed in the outcome admission ledger.

3.10. Expanded-Population Left Atrial Deformation

Expanded direct-data analyses suggested lower LA reservoir strain (four comparisons; 219 patients and 154 controls; MD −6.77 percentage points, 95% CI −11.15 to −2.38) and conduit strain (three comparisons; 155 patients and 104 controls; MD −7.20, 95% CI −11.89 to −2.50). These differences persisted with modified-HK inference.

Booster strain had an ordinary-HK MD of −1.40 percentage points (three comparisons; 183 patients and 112 controls; 95% CI −2.65 to −0.15), but the modified-HK interval included zero (−3.68 to 0.87). The expanded reservoir strain-rate model, including eligible converted observations, comprised three comparisons and was inconclusive (MD −0.279 s^{-1}, 95% CI −0.906 to 0.348). Huang W et al. [11] reported left atrial strain rate in %/s. The scale of the reported values could not be confirmed, so these data were retained as reported and excluded from pooling.

These secondary findings concern broader or incompletely documented populations. Reservoir, conduit, and booster measures were treated as separate physiological outcomes (Figures S22–S25).

Six cohort components contributed to the exploratory prognostic scope, and six quasi-experimental components contributed to the longitudinal treatment scope. The prognostic studies examined the associations between strain and subsequent clinical outcomes. The treatment studies reported changes in strain or strain rate during follow-up. Supplementary Table S6 presents the study-level findings for both scopes, which were summarised descriptively without pooling. A summary of findings for the principal left ventricular strain outcomes is presented in Table 2.

3.11. Exploratory Small-Study Effects

Exploratory Egger-type mixed-effects regression tests for small-study effects were performed for the expanded direct-data GLS (14 comparisons, $p = 0.379$) and GRS (10 comparisons, $p = 0.248$) analyses. The expanded GCS analysis and all principal analyses contained fewer than 10 comparisons and fell below the threshold for testing. The number of comparisons and clinical and measurement heterogeneity limited interpretation of the tests. Funnel plots for the expanded GLS and GRS analyses are presented in Figures S26 and S27.

Table 2. Summary of findings for the principal left ventricular strain outcomes. Question: How do CMR-derived LV strain measurements differ between patients with autoimmune rheumatic diseases with documented absence of clinically overt cardiac involvement and healthy controls? Setting: Clinical and research cohorts undergoing CMR. The comparisons were cross-sectional; no longitudinal clinical outcome was pooled. Mean differences are disease minus control, in percentage points. All three principal outcomes were designated important.

Outcome	Comparisons	Patients/ Controls	MD, Ordinary-HK 95% CI, Percentage Points	Modified-HK 95% CI	Certainty	Downgrade
LV GLS	5	168/130	+2.46 [0.82, 4.11]	0.82 to 4.11	Very low	Risk of bias, inconsistency, indirectness
LV GCS	4	140/102	+0.91 [−1.31, 3.12]	−1.38 to 3.19	Very low	Risk of bias, indirectness, serious imprecision (−1 level)
LV GRS	4	140/102	−1.42 [−4.80, 1.96]	−5.27 to 2.43	Very low	Risk of bias, indirectness, serious imprecision (−1 level)

Note: Mean differences (MDs) are disease minus control, in percentage points. The primary confidence intervals use ordinary Hartung–Knapp (HK) inference. Modified-HK inference sets a lower bound of one on the variance multiplier. The ordinary and modified Hartung–Knapp intervals coincide for GLS because its Hartung–Knapp scale factor was at least one. The modified method widened the GCS and GRS intervals. The certainty assessment concerns the direction of the average unadjusted association relative to zero. All three outcomes were downgraded for risk of bias and indirectness. GLS was additionally downgraded for inconsistency, and GCS and GRS were additionally downgraded for imprecision. Participant totals overlap across outcomes. CI, confidence interval; GLS, global longitudinal strain; GCS, global circumferential strain; GRS, global radial strain; MD, mean difference. All contributing evidence was non-randomised. Positive GLS/GCS differences represent less negative strain; a negative GRS difference represents lower radial strain.

3.12. Certainty of Evidence Results

Certainty was very low for GLS, GCS and GRS. We downgraded all three outcomes for risk of bias and indirectness. We additionally downgraded GLS for inconsistency and downgraded GCS and GRS by one level each for imprecision. For both outcomes, the modified Hartung–Knapp confidence interval crossed zero and allowed associations in either direction. The risk-of-bias downgrade reflected limitations in recruitment and comparator selection, residual confounding in the unadjusted comparisons, and uncertainty about strain measurement or statistical analysis in several reports. Supplementary Table S1 presents the item-level JBI judgements for the five reports contributing to the principal analyses. Supplementary Table S2 presents the outcome-level GRADE judgements and the rationale for each downgrade.

4. Discussion

4.1. Principal Findings

In the principal analysis, GLS was 2.46 percentage points less negative on average in the disease groups, but the evidence was very uncertain. The prediction interval included zero, and the confidence interval included zero after omitting Puntmann et al. [12]. The GCS and GRS confidence intervals allowed differences in either direction. The expanded analyses included a broader clinical population and are interpreted in that context.

4.2. Secondary Findings and Measurement Considerations

Sparse strain-rate and right-heart evidence limited pooled inference. The ordinary-HK diastolic radial strain-rate result did not remain directional with modified inference. Similarly, the expanded LA booster-strain result was sensitive to the HK modification,

whereas reservoir and conduit associations persisted. These findings emphasise the need to identify the population, measurement definition and inference method associated with each secondary result.

Regional, tagging, restricted-view, annular and three-dimensional measurements were retained separately. Similar terminology does not establish measurement equivalence, and standardised effects cannot by themselves resolve differences between acquisition methods or analysis platforms.

Clinical eligibility and CMR tissue findings captured different aspects of cardiac involvement. Late gadolinium enhancement was present in 28 of 47 patients in the Kersten idiopathic inflammatory myopathy cohort [15], and in nine of 30 patients assessed for enhancement in the Ross systemic sclerosis cohort [7]. Ross et al. also reported ventricular ectopy in 17 patients (54.8%) [7]. The two LGE-negative GLS comparisons were imprecise, and both confidence intervals included zero. These findings leave uncertainty about whether the pooled GLS association extends to patients without detectable LGE.

4.3. Clinical Interpretation

The findings describe average unadjusted differences between groups. Their relevance to individual diagnosis, prognosis or screening remains uncertain. Future studies should recruit disease-specific cohorts, define clinical and imaging phenotypes prospectively, and report scanner field strength, cine acquisition views, analysis software and version, and strain definitions. Longitudinal follow-up should assess whether deformation measures are associated with patient-important outcomes.

4.4. Strengths and Limitations

The revision expanded the search to include Web of Science, repeated selection, and distinguished report inclusion from outcome admission, and separated clinical phenotypes and measurement constructs. Shared controls and possible cohort overlap were handled explicitly, and numerical holds, conversions and alternative inference methods were documented.

The principal models included five GLS comparisons and four comparisons each for GCS and GRS. Comparator selection, residual confounding and differences in measurement methods limited interpretation of the unadjusted group differences. Minimum age could not be verified explicitly for most contributing cohorts. The restriction to explicitly verified adult eligibility yielded one GLS comparison, and the LGE-negative restriction yielded two GLS comparisons. These sets fell below the revised pooling threshold.

Technical and population heterogeneity remained. Possible cohort relationships were handled conservatively without assuming participant identity that was not demonstrated. Median/IQR conversion cannot reconstruct original distributions, and withholding inconsistent or nonseparable outcomes limited coverage. Exploratory small-study diagnostics were available only for expanded models and do not exclude publication bias.

Several analytical policies and the GRADE certainty target were clarified during revision. The supplementary records distinguish reviewer agreement recorded during the initial review, agreement confirmed during revision, AI-assisted checks, and computational validation.

5. Conclusions

The pooled GLS estimate suggested a smaller magnitude of longitudinal shortening in patients with autoimmune rheumatic diseases without established clinically overt cardiac disease, but the evidence was very uncertain. The prediction interval included zero. Evidence for circumferential and radial strain was also of very low certainty, with confi-

dence intervals allowing differences in either direction. The LGE-negative and explicitly age-verified subsets were too sparse for pooling under the revised analysis rule.

Supplementary Materials: The following supporting information can be downloaded at: https://www.mdpi.com/article/10.3390/biomedicines14112666/s1. The Supplementary Materials include the complete database search strategies and the Europe PMC citation search methods and record counts (Supplementary Search Strategies and Audit); characteristics and bibliographic references for all 73 retained reports; the full-text exclusion register with primary exclusion reasons; the register of reports not retrieved; baseline and design-specific JBI appraisal records and the item-level appraisal of the five principal reports (Supplementary Table S1); the GRADE evidence profile (Supplementary Table S2); the principal GLS leave-one-out analysis (Supplementary Table S3); the individual GLS estimates under the LGE and adult-age restrictions (Supplementary Table S4); the review amendments (Supplementary Table S5), the study-level prognostic and longitudinal treatment findings (Supplementary Table S6), the numerical input verification log; and supplementary outcome and sensitivity figures. Figures S1–S25 present supplementary outcome forest plots. Figures S26 and S27 present exploratory funnel plots for the expanded direct-data LV GLS and GRS analyses, respectively. A completed PRISMA 2020 [17] checklist is also provided. The extraction dataset, report-selection decision log, outcome admission ledger, model membership and model results files, conversion audit, and analysis code are deposited separately in Zenodo.

Author Contributions: Conceptualisation: D.-A.A., S.-F.A. and S.P.; Methodology: D.-A.A., S.-F.A. and M.T.; Software: S.-F.A. and M.T.; Validation: D.-A.A., S.-F.A., M.T., D.M. and S.P.; Formal analysis: D.-A.A., S.-F.A. and M.T.; Investigation: D.-A.A., S.-F.A., R.T., S.M. and S.O.; Data curation: D.-A.A., S.-F.A., Z.A., R.J. and C.S.; Writing—original draft preparation: D.-A.A., S.-F.A., M.T., R.T., S.M. and S.O.; Writing—review and editing: M.T., Z.A., R.J., C.S., T.A., A.-M.P., R.I.L., V.M., B.C.B., C.M., C.V., D.C., D.M., S.I., M.A., O.M.C. and S.P.; Visualisation: D.-A.A., S.-F.A., M.T. and T.A.; Supervision: S.P., O.M.C. and M.A.; Project administration: D.-A.A., S.-F.A. and S.P. All authors have read and agreed to the published version of the manuscript.

Funding: This research received no external funding. The article processing charge will be paid by Victor Babeș University of Medicine and Pharmacy, Timișoara, Romania.

Institutional Review Board Statement: Ethical review and approval were not required because this study was a systematic review and meta-analysis of previously published aggregate data and involved no new collection of identifiable participant information.

Informed Consent Statement: Not applicable.

Data Availability Statement: The final study-level extraction dataset, report-selection decision log, outcome admission ledger, model membership and model results files, conversion audit, and analysis code are openly available in Zenodo at https://doi.org/10.5281/zenodo.24150247. Critical appraisal records, GRADE evidence profiles, search strategies, and supplementary figures are provided with the article as Supplementary Materials.

Acknowledgments: AI assistance was used to support extraction preparation, eligibility assessment and preliminary item-level appraisal during the initial review. During revision, OpenAI ChatGPT 5.6 Sol was used to support source cross-checking, structured data and numerical checks, statistical code and output checks, and limited language editing. The exact historical ChatGPT model versions could not be established from the retained records. Sections 2.4, 2.5, 2.8 and 3.3 describe the respective roles of the reviewers and AI assistance and the scope of the available verification records. The authors take responsibility for the review decisions and submitted manuscript.

Conflicts of Interest: The authors declare no conflicts of interest.

Abbreviations

The following abbreviations are used in this manuscript:

ARD	Autoimmune rheumatic disease
CENTRAL	Cochrane Central Register of Controlled Trials
CI	Confidence interval
CMR	Cardiovascular magnetic resonance
GCS	Global circumferential strain
GLS	Global longitudinal strain
GRADE	Grading of Recommendations Assessment, Development and Evaluation
GRS	Global radial strain
IIM	Idiopathic inflammatory myopathy
IQR	Interquartile range
JBI	Joanna Briggs Institute
LA	Left atrial
LGE	Late gadolinium enhancement
LV	Left ventricular
LVEF	Left ventricular ejection fraction
MD	Mean difference
PRISMA	Preferred Reporting Items for Systematic Reviews and Meta-Analyses
PROSPERO	International Prospective Register of Systematic Reviews
pSS	Primary Sjögren syndrome
RA	Rheumatoid arthritis
REML	Restricted maximum likelihood
SLE	Systemic lupus erythematosus
SSc	Systemic sclerosis

References

1. Prasad, M.; Hermann, J.; Gabriel, S.E.; Weyand, C.M.; Mulvagh, S.; Mankad, R.; Oh, J.K.; Matteson, E.L.; Lerman, A. Cardiorheumatology: Cardiac involvement in systemic rheumatic disease. *Nat. Rev. Cardiol.* **2015**, *12*, 168–176. [CrossRef] [PubMed]
2. De Zorzi, E.; Spagnolo, P.; Cocconcelli, E.; Balestro, E.; Iaccarino, L.; Gatto, M.; Benvenuti, F.; Bernardinello, N.; Doria, A.; Maher, T.M.; et al. Thoracic Involvement in Systemic Autoimmune Rheumatic Diseases: Pathogenesis and Management. *Clin. Rev. Allergy Immunol.* **2022**, *63*, 472–489. [CrossRef] [PubMed]
3. Casian, M.; Dima, A.; Jurcuț, C.; Andrei, L.; Edwards, J.; O'Driscoll, J.; Popescu, B.A.; Jurcuț, R. Cardiac function and mechanics in systemic sclerosis: A systematic review and meta-analysis. *Echo Res. Pract.* **2025**, *12*, 18. [CrossRef] [PubMed]
4. Rajiah, P.S.; Kalisz, K.; Broncano, J.; Goerne, H.; Collins, J.D.; François, C.J.; Ibrahim, E.-S.; Agarwal, P.P. Myocardial Strain Evaluation with Cardiovascular MRI: Physics, Principles, and Clinical Applications. *Radiographics* **2022**, *42*, 968–990. [CrossRef] [PubMed]
5. Bratis, K.; Lindholm, A.; Hesselstrand, R.; Arheden, H.; Karabela, G.; Stavropoulos, E.; Katsifis, G.; Kolovou, G.; Kitas, G.D.; Sfikakis, P.P.; et al. CMR feature tracking in cardiac asymptomatic systemic sclerosis: Clinical implications. *PLoS ONE* **2019**, *14*, e0221021. [CrossRef] [PubMed]
6. Peng, Y.; He, H.; Tong, X.; Liu, B.; Shao, W.; Xu, D.; Zhao, X.; Ding, H.; Lai, J.; He, Z.-X. Association between myocardial involvement and subclinical left ventricular dysfunction in patients with systemic sclerosis: A cardiac magnetic resonance study. *Quant. Imaging Med. Surg.* **2026**, *16*, 458. [CrossRef] [PubMed]
7. Ross, L.; Costello, B.; Brown, Z.; Hansen, D.; Lindqvist, A.; Stevens, W.; Burns, A.; Prior, D.; Nikpour, M.; La Gerche, A. Myocardial fibrosis and arrhythmic burden in systemic sclerosis. *Rheumatology* **2022**, *61*, 4497–4502. [CrossRef] [PubMed]
8. Palumbo, P.; Ruscitti, P.; Cannizzaro, E.; Berardicurti, O.; Conforti, A.; Di Cesare, A.; Di Cola, I.; Giacomelli, R.; Splendiani, A.; Barile, A.; et al. Unenhanced Cardiac Magnetic Resonance may improve detection and prognostication of an occult heart involvement in asymptomatic patients with systemic sclerosis. *Sci. Rep.* **2022**, *12*, 5125. [CrossRef] [PubMed]
9. Ntusi, N.A.B.; Piechnik, S.K.; Francis, J.M.; Ferreira, V.M.; Rai, A.B.S.; Matthews, P.M.; Robson, M.D.; Moon, J.; Wordsworth, P.B.; Neubauer, S.; et al. Subclinical myocardial inflammation and diffuse fibrosis are common in systemic sclerosis—A clinical study using myocardial T1-mapping and extracellular volume quantification. *J. Cardiovasc. Magn. Reson.* **2014**, *16*, 21. [CrossRef] [PubMed]
10. Huang, L.; Wang, X.; Yuan, Y.; Wu, A.; Tang, L.; Huang, C.; Yu, L.; Lin, Q. Evaluation of subclinical myocardial involvement in systemic lupus erythematosus using multiparametric cardiac magnetic resonance imaging. *BMC Cardiovasc. Disord.* **2025**, *25*, 597. [CrossRef] [PubMed]

11. Huang, W.; Dong, J.; Luo, S.; Zhang, J.; Zhang, L.; Ma, Y.; Wang, B.; Wang, J.; Dou, W.; Qi, L.; et al. Cardiac magnetic resonance feature tracking evaluates left atrial strain in patients with systemic lupus erythematosus and mitral regurgitation. *Lupus* **2025**, *34*, 799–809. [CrossRef] [PubMed]
12. Puntmann, V.O.; D'Cruz, D.; Smith, Z.; Pastor, A.; Choong, P.; Voigt, T.; Carr-White, G.; Sangle, S.; Schaeffter, T.; Nagel, E. Native myocardial T1 mapping by cardiovascular magnetic resonance imaging in subclinical cardiomyopathy in patients with systemic lupus erythematosus. *Circ. Cardiovasc. Imaging* **2013**, *6*, 295–301. [CrossRef] [PubMed]
13. Tański, W.; Gać, P.; Chachaj, A.; Mazur, G.; Poręba, R.; Szuba, A. Left ventricular myocardial strain assessed by cardiac magnetic resonance feature tracking in patients with rheumatoid arthritis. *Insights Imaging* **2021**, *12*, 5. [CrossRef] [PubMed]
14. Yokoe, I.; Kobayashi, H.; Nishiwaki, A.; Nagasawa, Y.; Kitamura, N.; Haraoka, M.; Kobayashi, Y.; Takei, M.; Nakamura, H. Asymptomatic myocardial dysfunction was revealed by feature tracking cardiac magnetic resonance imaging in patients with primary Sjögren's syndrome. *Int. J. Rheum. Dis.* **2021**, *24*, 1482–1490. [CrossRef] [PubMed]
15. Kersten, J.; Güleroglu, A.M.; Rosenbohm, A.; Buckert, D.; Ludolph, A.C.; Hackenbroch, C.; Beer, M.; Bernhardt, P. Myocardial involvement and deformation abnormalities in idiopathic inflammatory myopathy assessed by CMR feature tracking. *Int. J. Cardiovasc. Imaging* **2021**, *37*, 597–603. [CrossRef] [PubMed]
16. Qiao, W.; Bi, W.; Wang, X.; Li, Y.; Ren, W.; Xiao, Y. Cardiac involvement assessment in systemic sclerosis using speckle tracking echocardiography: A systematic review and meta-analysis. *BMJ Open* **2023**, *13*, e063364. [CrossRef] [PubMed]
17. Page, M.J.; McKenzie, J.E.; Bossuyt, P.M.; Boutron, I.; Hoffmann, T.C.; Mulrow, C.D.; Shamseer, L.; Tetzlaff, J.M.; Akl, E.A.; Brennan, S.E.; et al. The PRISMA 2020 statement: An updated guideline for reporting systematic reviews. *BMJ* **2021**, *372*, n71. [CrossRef] [PubMed]
18. Luo, D.; Wan, X.; Liu, J.; Tong, T. Optimally estimating the sample mean from the sample size, median, mid-range, and/or mid-quartile range. *Stat. Methods Med. Res.* **2018**, *27*, 1785–1805. [CrossRef] [PubMed]
19. Wan, X.; Wang, W.; Liu, J.; Tong, T. Estimating the sample mean and standard deviation from the sample size, median, range and/or interquartile range. *BMC Med. Res. Methodol.* **2014**, *14*, 135. [CrossRef] [PubMed]
20. Moola, S.; Munn, Z.; Tufanaru, C.; Aromataris, E.; Sears, K.; Sfetcu, R.; Currie, M.; Lisy, K.; Qureshi, R.; Mattis, P.; et al. Chapter 7: Systematic reviews of etiology and risk. In *JBI Manual for Evidence Synthesis*; Aromataris, E., Munn, Z., Eds.; JBI: Adelaide, Australia, 2020. [CrossRef]
21. Viechtbauer, W. Conducting Meta-Analyses in R with the metafor Package. *J. Stat. Softw.* **2010**, *36*, 1–48. [CrossRef]
22. IntHout, J.; Ioannidis, J.P.A.; Borm, G.F. The Hartung-Knapp-Sidik-Jonkman method for random effects meta-analysis is straightforward and considerably outperforms the standard DerSimonian-Laird method. *BMC Med. Res. Methodol.* **2014**, *14*, 25. [CrossRef] [PubMed]
23. Röver, C.; Knapp, G.; Friede, T. Hartung-Knapp-Sidik-Jonkman approach and its modification for random-effects meta-analysis with few studies. *BMC Med. Res. Methodol.* **2015**, *15*, 99. [CrossRef] [PubMed]
24. Guyatt, G.; Oxman, A.D.; Akl, E.A.; Kunz, R.; Vist, G.; Brozek, J.; Norris, S.; Falck-Ytter, Y.; Glasziou, P.; DeBeer, H.; et al. GRADE guidelines: 1. Introduction—GRADE evidence profiles and summary of findings tables. *J. Clin. Epidemiol.* **2011**, *64*, 383–394. [CrossRef] [PubMed]
25. Guyatt, G.; Zeng, L.; Brignardello-Petersen, R.; Prasad, M.; De Beer, H.; Murad, M.H.; Iorio, A.; Agarwal, A.; Yao, L.; Agoritsas, T.; et al. Core GRADE 2: Choosing the target of certainty rating and assessing imprecision. *BMJ* **2025**, *389*, e081904. [CrossRef] [PubMed]
26. Brignardello-Petersen, R.; Guyatt, G.H. Assessing the certainty of the evidence in systematic reviews: Importance, process, and use. *Am. J. Epidemiol.* **2025**, *194*, 1681–1686. [CrossRef] [PubMed]
27. Treiber, J.M.; Wilhelmi, T.; Binz, C.; Backhaus, S.J.; Wolter, S.; Rieth, A.; Rademann, M.; Kriechbaum, S.; Müller-Ladner, U.; Sossalla, S.; et al. Myocardial inflammatory activity and structural injury are discordant in connective tissue disease compared with acute suspected viral myocarditis: A CMR study. *Clin. Res. Cardiol.* **2026**. [CrossRef] [PubMed]
28. Zhao, P.; Huang, L.; Ran, L.; Tang, D.; Zhou, X.; Xia, L. CMR T1 mapping and strain analysis in idiopathic inflammatory myopathy: Evaluation in patients with negative late gadolinium enhancement and preserved ejection fraction. *Eur. Radiol.* **2021**, *31*, 1206–1215. [CrossRef] [PubMed]

Disclaimer/Publisher's Note: The statements, opinions and data contained in all publications are solely those of the individual author(s) and contributor(s) and not of MDPI and/or the editor(s). MDPI and/or the editor(s) disclaim responsibility for any injury to people or property resulting from any ideas, methods, instructions or products referred to in the content.